Comparison Between 180° and 360° Data Collection in Technetium-99m MIBI SPECT of the Myocardium

Jean C. Maublant, Patricia Peycelon, Fabrice Kwiatkowski, Jean-René Lusson, Rüdiger H. Standke, and Annie Veyre

Centre Jean Perrin and University Hospital, Clermont-Ferrand, France and Goethe-University Hospital, Frankfurt, FRG

In a series of 12 patients presenting with a single-vessel coronary artery disease and who were injected with 370 MBq of ^{99m}Tc-2-methoxyisobutylisonitrile at peak exercise, two consecutive single photon emission computed tomography (SPECT) data collections, i.e., 32 views of 30 sec during a 180° rotation and 64 views of 15 sec during a 360° rotation, were performed 1 hr later. In both cases, transverse sections were reconstructed using (a) a backprojection method with a ramp filter, (b) a correction for downscatter, (c) a correction for depth attenuation by the Chang method, or (d) both corrections. Each reconstructed myocardium was then divided into four short-axis sections which were radially divided into nine sectors. Sectors with an activity below 80% of the maximum were considered as abnormal. Sensitivity and specificity were calculated relative to a sector-by-sector theoretical anatomic distribution of the perfusion abnormalities. Results demonstrate that, of all situations, the best balance between sensitivity and specificity was achieved with the 180° data collection and no correction at reconstruction. Using the 360° data sampling technique mainly lowered the sensitivity in the patients with a circumflex or right coronary artery disease. It is concluded that there does not seem to be any definite advantage in performing a 360° rather than a 180° data collection in ^{99m}Tc myocardial SPECT.

J Nucl Med 30:295–300, 1989

Technetium-99m- (^{99m}Tc) labeled isonitriles have been recently proposed as an alternative to thallium-201 (^{201}Tl) chloride for myocardial blood flow imaging (*1*). In ^{201}Tl myocardial single photon emission computed tomography (SPECT) the acquisition is usually performed using a 180° data collection, although there is still some controversy about its superiority as compared to a 360° data collection (*2–10*). This controversy has not yet extended to ^{99m}Tc myocardial SPECT, although since the energy of photon emission of ^{99m}Tc is higher than ^{201}Tl, it could be hypothetized that the 360° mode is preferable to the 180° mode. In order to test this hypothesis, both modes were compared in a series of 12 patients using an objective method.

MATERIALS AND METHODS

Twelve patients of mean age 53 yr (range 36–66 yr) including ten males and two females were involved in the study. It was approved by the local Committee of Ethics and patients were informed. All patients had single-vessel coronary artery disease (CAD) documented by a contrast coronary angiography performed within 3 wk of the scintigraphic examination. Six patients presented with significant stenosis, i.e., over 70% narrowing of the lumen, of the left anterior descending (LAD) coronary artery, six others of the circumflex or right coronary artery (RCA). At peak exercise during a stress test on a bicycle, a 10 mCi (370 MBq) dose of ^{99m}Tc-2-methoxyisobutylisonitrile (MIBI) (Cardiolite, DuPont Diagnostic Imaging Division, North Bellerica, MA) was injected intravenously when the maximal theoretical heart rate was attained or when the test was becoming positive.

Exercise was sustained for an additional minute after injection. One hour later, two independent SPECT data collections, one with a 180° rotation and one with a 360° rotation, were performed sequentially. The 180° data collection was performed before the 360° one in four patients, and vice versa in eight patients. The scintillation camera (Gammatome II, Sopha, Buc, France) was equipped with a low-energy, high resolution, parallel hole collimator. The spectrometer was set on two different windows. One had a 20% width and was centered on the 140-keV gamma peak of ^{99m}Tc. The other window had a 40% width and was positioned on the Compton peak. The average count ratio between the two resulting

Received Mar. 1, 1988; revision accepted Sept. 21, 1988.

For reprints contact: J.C. Maublant, MD, Centre Jean Perrin, 63011 Clermont-Ferrand, France.

images (primary photopeak/Compton peak) was 1.2. These two images were stored separately as 64 × 64 matrices in a dedicated computer (S4000, Sopha, Buc, France). In the 180° mode, the acquisition was performed between the left posterior oblique and right anterior oblique projections. In this mode, 32 views of 30-sec each were collected. In the 360° mode, 64 views of 15-sec each were acquired. In both modes, the head of the camera followed a similar circular orbit. Great care was taken not to move the patient or to change the radius of rotation of the camera between the two acquisitions.

Each acquisition was processed in four different ways using a commercially available software.

1. A backprojection using the images corresponding to the 140-keV gamma peak was applied with a pure ramp filter (this option will be referred below as the standard method).

2. A downscatter correction was performed by subtracting from the standard sections 50% of the activity of the sections reconstructed with the Compton peak (*11*).

3. A correction for attenuation was applied using the Chang method (*12*), i.e., by fitting an ellipse around the thorax and applying a 0.12 cm^{-1} attenuation coefficient.

4. Both corrections for scatter and depth attenuation were applied, with a 0.15 cm^{-1} attenuation coefficient. All series were smoothed after reconstruction (*13*).

The effects of the corrections have been previously assessed with a cylindrical phantom filled with [^{99m}Tc]pertechnetate. Figure 1 shows that downscatter alone does not affect significantly the uncorrected profile of activity. Attenuation correction increases the activity near the center but does not properly flatten the periphery of the profile. Although this effect could be due to statistical fluctuation or incorrect setting of the ellipse, the addition of scatter correction results in an almost rectangular transition at the periphery of the cylinder which is, in the thorax, the area that contains the myocardium. These effects are similar with the 180° and 360° data collections.

Since both the 180° and 360° data collections were processed the same way, it resulted in the reconstruction for each patient of eight series of adjacent one-pixel-thick transverse sections. The upper and lower limits of reconstruction of these series were identical in a given patients, resulting in a constant number of transverse sections in the eight series. This number ranged between 12 and 16 in our population. For the 3 and 4 reconstructions, the limits of the elliptical contour were manually selected once for a given patient and kept constant.

In order to compare as objectively as possible these series, we used a commercially available semiautomatic quantitative method (Sophy, Sopha, Buc, France) which was applied to the eight series of the 12 patients using the same parameters and resulting in an observer-free comparison. In this method, the long axis of the heart is reoriented along the vertical and horizontal planes and the anterior and posterior limits of the left ventricular myocardium are manually selected. The myocardium is then automatically divided into four adjacent short axis slices. Each slice was submitted to a circumferential uptake analysis within nine sectors, resulting in a 36-sector analysis per series (*14*). The mean activity per sector was normalized to the maximum of the series. A sector was considered normal if its activity was >80% of maximal and abnormal otherwise.

An "anatomic map" of the most likely distribution of the abnormal sectors was drawn for the three main coronary artery territories, i.e., the LAD coronary artery, the circumflex, and

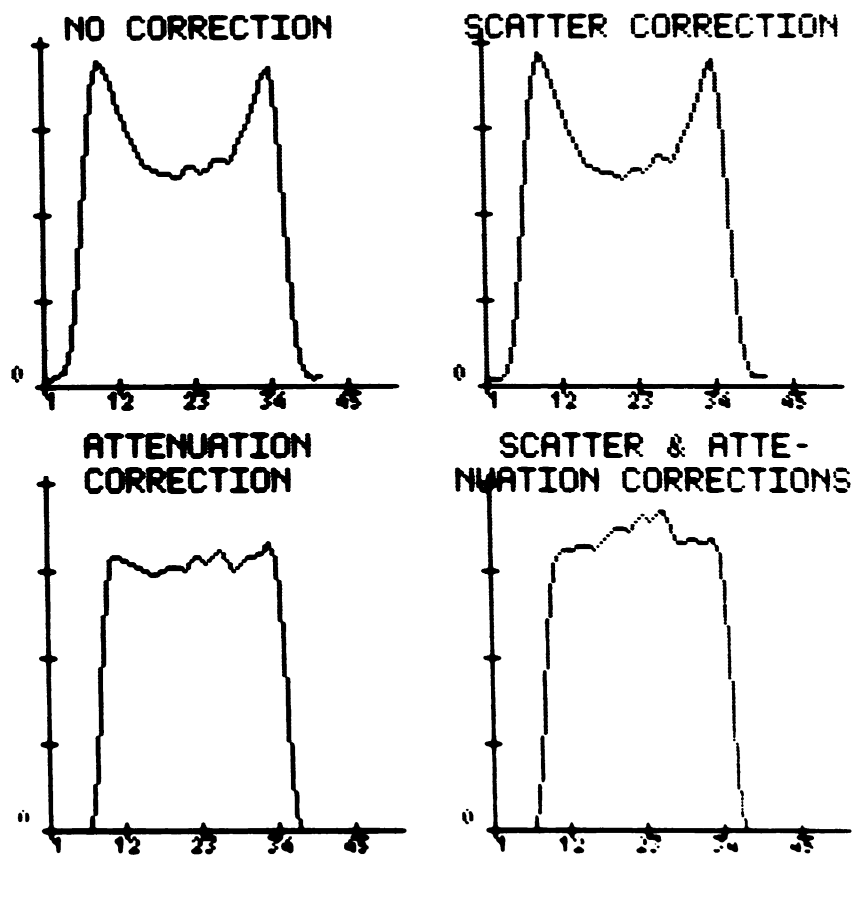

FIGURE 1
Effects of corrections on a profile of activity passing through a transverse section of a cylinder filled with [^{99m}Tc] pertechnetate. All curves are normalized to their own maximum.

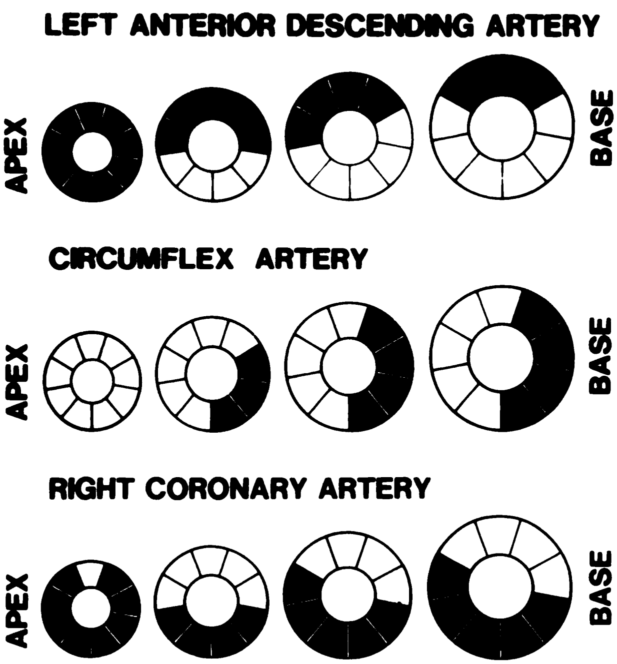

FIGURE 2
"Anatomic map" showing the ideal territories of the three main coronary arteries (black sectors) on short-axis sections.

the RCA (Fig. 2). In each patient the actual distribution of the normal and abnormal sectors was compared with the distribution of the sectors on the "anatomic map" corresponding to the stenosed coronary artery.

Sensitivity and specificity were calculated as: (total number of abnormal sectors at tomography)/(total number of abnormal sectors on the "anatomic map"), and (total number of normal sectors at tomography)/(total number of normal sectors on the "anatomic map"), respectively.

Results are presented as mean ± s.d. When necessary, comparisons were made by the chi-square test. Differences were considered significant when below the 5% confidence level.

RESULTS

Table 1 shows that sensitivity ranges between 48% and 84%, and specificity between 38% and 70%. In the overall population, sensitivity is always slightly lower in the 360° than in the 180° modes. However, when subgroups are considered, sensitivity is always higher in the anterior than in the inferior lesions. This difference is larger in the 360° than in the 180° rotation modes, mostly because the sensitivity for the inferior lesions dramatically drops in the 360° mode. Specificity is higher in the 360° mode, except in the dual corrections mode (differences are not significant).

Looking more specifically at the sensitivity of the dual corrections method as compared with the standard mode, the former generally has a higher sensitivity in either the 180° or 360° modes. Both specificities are close to each other in the 180° mode, but it is lower for the dual corrections method in the 360° mode (70% vs. 44%, $p < 0.001$), mainly for the inferior lesions (69% vs. 38%, $p < 0.001$). The mean number of normal sectors with the standard reconstruction mode is slightly higher in the 360° than in the 180° technique (25.6 ± 3.5 vs. 23.9 ± 2.9, N.S., respectively). There is also a

TABLE 1
Sensitivity and Specificity of the 180° and 360° Collections Using Four Reconstruction Modes

Reconstruction mode	Location of CAD	180° Collection Sensitivity	180° Collection Specificity	360° Collection Sensitivity	360° Collection Specificity
Standard Reconstruction	Ant*	68	56	71	67
	Inf†	60	64	48	69
	All	63	59	58	70
With downscatter correction	Ant	74	42	78	60
	Inf	65	60	50	62
	All	69	48	62	61
With correction for attenuation	Ant	79	58	79	64
	Inf	59	55	55	52
	All	68	57	66	60
With both corrections	Ant	79	60	84	47
	Inf	64	45	56	38
	All	71	54	69	44

* Territory of the left anterior descending coronary artery.
† Territory of the circonflexe and right coronary arteries.

moderate difference with the dual corrections method (19.1 ± 5.0 vs. 18.2 ± 3.8, N.S., respectively). However, when compared with the 180° rotation, the specificity of the 360° rotation is higher with the standard reconstruction (70% vs. 59%, $p < 0.10$) and lower with the dual corrections. As in the other situation, sensitivity is lower in the 360° than 180° rotations. Therefore, the changes in sensitivity and specificity encountered between the 360° and 180° modes are different with the standard reconstruction and with the dual corrections reconstruction. The smallest changes are obtained with the standard reconstruction.

Tables 2, 3, and 4 show the consequences, on the tracer distribution, of a 360° data collection, of scatter correction and of attenuation correction when compared with a 180° data collection and standard reconstruction. Figure 3 shows the sector-by-sector distribution of the positive and negative differences of activity. It appears that the scatter correction tends to increase the activity in the septal and inferior walls, while the attenuation correction increases the activity in the two most basal sections. The latter effect can be simply explained by the fact that the base of the heart is more deeply situated in the thorax and is therefore more corrected than the rest of the myocardium.

DISCUSSION

The comparison between the 180° and 360° data collection performed in 12 patients did not demonstrate any advantage of performing a 360° rather than a 180° data collection. Because of the relatively small number of patients involved in the study, most of the changes in sensitivity and specificity were not statistically significant. However, even if the differences were significant, it would not make the 360° data sampling technique superior to the 180° one since the best balance between sensitivity and specificity for the detection of abnormal sectors was achieved with the 180° data sampling technique and no correction at reconstruction.

Several studies have already addressed the same topic but with ^{201}Tl instead of ^{99m}Tc as a myocardial imaging agent (*2–10*). It seems that the 360° data collection could introduce some image distorsion (*7*). The objection of limited-angle sampling that could invalidate the 180° data collection (*7*) is not truly relevant since in the 360° technique the opposite views are added by arithmetic or geometric mean, which means that the angle of view is theoretically the same in both situations. The quality of the myocardial image is always by far

TABLE 3
Average Sector-by-Sector Differences of Activity Between the 180° Standard Mode and the 180° Scatter Correction Mode*

Sector no.	Section 1	Section 2	Section 3	Section 4
1	0.1 ± 1.3	−0.4 ± 1.8	1.1 ± 2.1	1.9 ± 1.9†
2	0.1 ± 1.1	−0.4 ± 1.5	0.0 ± 1.5	1.1 ± 1.8
3	1.1 ± 1.6†	0.6 ± 1.5	0.3 ± 1.4	0.5 ± 1.2
4	3.1 ± 3.0‡	2.1 ± 3.1†	1.8 ± 2.4†	1.5 ± 1.9†
5	6.4 ± 4.1§	4.9 ± 3.7§	3.8 ± 3.5‡	2.4 ± 3.0†
6	7.1 ± 4.3§	6.4 ± 4.1§	4.3 ± 3.2§	3.1 ± 3.0‡
7	5.5 ± 4.2§	4.4 ± 3.2‡	3.0 ± 2.5‡	2.4 ± 1.9§
8	2.3 ± 1.9§	1.4 ± 1.4‡	0.8 ± 1.1†	1.3 ± 1.1‡
9	0.4 ± 1.0	−0.1 ± 1.4	0.3 ± 1.5	1.6 ± 1.4‡

*Values are expressed in percent of activity relative to the maximal activity of each series (m ± s.d.).
† $p < 0.05$.
‡ $p < 0.01$.
§ $p < 0.001$.

TABLE 2
Average Sector-by-Sector Differences of Activity Between the 180° Standard and 360° Standard Modes*

Sector no.	Section 1	Section 2	Section 3	Section 4
1	−0.3 ± 8.1	−2.9 ± 5.9	−1.1 ± 7	3.8 ± 8.0
2	0.9 ± 11.6	1.7 ± 6.8	−0.8 ± 5	−1.5 ± 6.6
3	−0.9 ± 11.3	2.1 ± 6.0	0.0 ± 5.2	−3.7 ± 7.3
4	2.8 ± 9.2	0.1 ± 5.3	−1.6 ± 5.7	−3.6 ± 6.7
5	4.1 ± 8.4	2.9 ± 6.5	−3.8 ± 5.7†	−1.6 ± 7.5
6	−0.1 ± 10.6	−5.4 ± 5.5‡	−3.9 ± 4.1‡	0.5 ± 7.3
7	−1.1 ± 8.6	−3.1 ± 6.1	−0.4 ± 5.0	0.6 ± 6.2
8	−2.8 ± 6.8	−1.4 ± 6.6	1.0 ± 7.1	0.9 ± 6.7
9	−4.9 ± 6.7†	−4.1 ± 5.4†	1.5 ± 8.3	3.8 ± 9.6

*Values are expressed in percent of activity relative to the maximal activity of each series (m ± s.d.).
† $p < 0.05$.
‡ $p < 0.01$.

TABLE 4
Average Sector-by-Sector Differences of Activity Between the 180° Standard Mode and the 180° Attenuation Correction Mode*

Sector no.	Section 1	Section 2	Section 3	Section 4
1	15.6 ± 3.7§	7.7 ± 4.2§	−2.7 ± 4.2†	−8.4 ± 3.9§
2	16.6 ± 4.2§	9.1 ± 3.9§	−1.6 ± 3.1	−7.1 ± 3.3§
3	15.8 ± 4.4§	9.1 ± 3.6§	−1.2 ± 2.9	−6.6 ± 3.3§
4	15.2 ± 4.3§	6.8 ± 3.4§	−2.4 ± 3.1†	−7.9 ± 3.9§
5	13.6 ± 4.0§	4.1 ± 3.3‡	−4.9 ± 3.4§	−9.5 ± 4.0§
6	13.2 ± 4.2§	2.5 ± 3.5†	−6.1 ± 3.1§	−10.0 ± 3.4§
7	15.1 ± 4.2§	4.1 ± 4.0‡	−5.4 ± 2.9§	−7.9 ± 2.4§
8	15.4 ± 4.3§	6.2 ± 4.3§	−4.6 ± 4.0‡	−6.4 ± 1.9§
9	14.4 ± 3.6§	7.2 ± 4.8§	−3.4 ± 4.6†	−7.5 ± 3.8§

*Values are expressed in percent of activity relative to the maximal activity of each series (m ± s.d.).
† $p < 0.05$.
‡ $p < 0.01$.
§ $p < 0.001$.

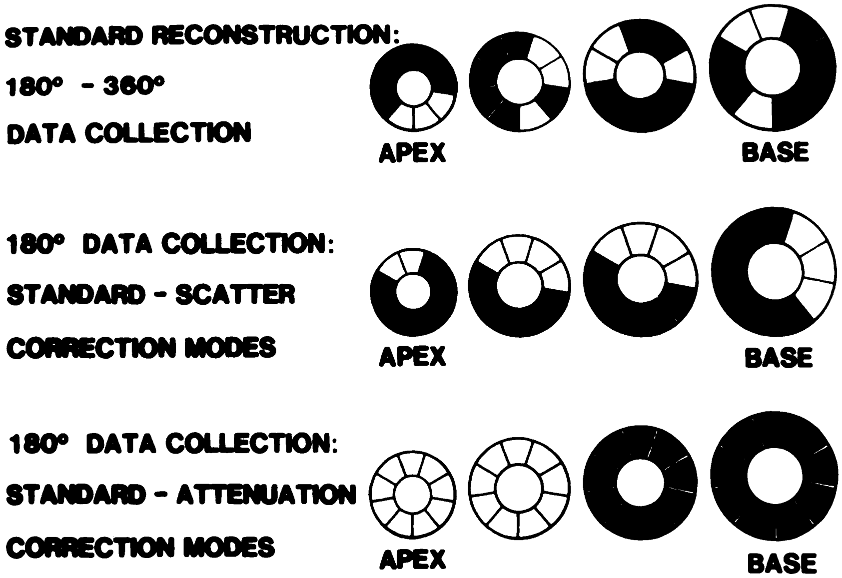

FIGURE 3
Effects of a 360° data collection (top), of scatter correction (middle) and of attenuation correction (bottom) when compared by subtraction with a 180° data collection and a standard reconstruction. Dark sectors reflect a negative difference value.

better with the 180° data sampling mode, mostly because of the lower background activity. Figure 4 clearly demonstrates that the same effect is observed with ^{99m}Tc. This comes from the fact that the 360° data collection brings in the series some images containing the activity present in the posterior part of the thorax, activity that is not detected during a 180° data collection. This phenomenon has been noticed early by Tamaki et al. (*15*).

In most of the former comparisons between 180° and 360° data collection, the duration of acquisition for the 180° technique was half of that for the 360° technique (*3,7,15*). This resulted in poorer statistics with the 180° mode and therefore in an unfair comparison about the actual quality of the pictures or the variability of the number of counts. Using the same duration of acquisition, which is what does count in the clinical situation, shows that there is no significant difference in [^{99m}Tc] MIBI SPECT.

Results in Table 1 demonstrate that the main disadvantage of the 360° data sampling technique is its dramatically low sensitivity in detecting the inferior lesions. It increases when the corrections are utilized at reconstruction, but then the specificity decreases, mostly because abnormalities appear on the anterior wall. It could be argued that specificity should be considered relative to the distribution of the activity as measured in a series of normal myocardium. This would likely decrease the number of false-positive sectors and, hence, increase the specificity, but the variations between the 180° and 360° data collection would remain the same. The sensitivity would either remain the same or decrease. Therefore, these results in the conditions of the study, do not show any advantage of the 360° collection in either mode of reconstruction.

Relative to the comfort of the patient, if one has to choose between a 180° and 360° data sampling technique, it seems preferable to perform a 180° rotation

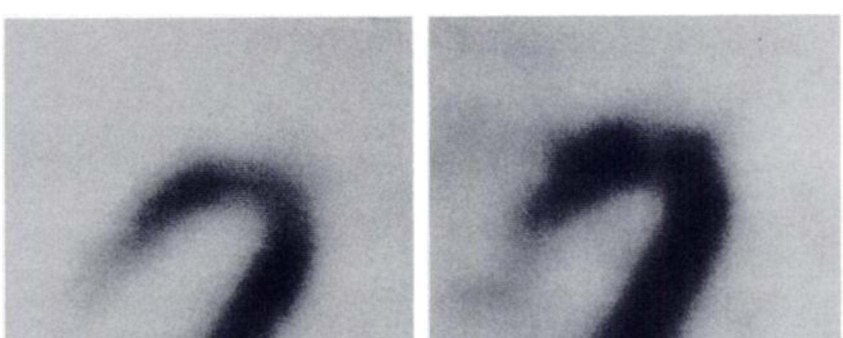

FIGURE 4
Transverse sections of the heart in a patient injected with [^{99m}Tc]MIBI. Data collection was performed over 180° (left) and 360° (right). Background activity is higher and myocardial walls are thicker with the 360° data sampling technique.

since the patient has only to keep his left arm over his head, instead of both arms. All these reasons suggest that it seems advisable to recommend a 180° data collection for [^{99m}Tc]MIBI SPECT of the myocardium.

ACKNOWLEDGMENTS

Cardiolite was kindly supplied by DuPont Diagnostic Imaging Division, North Bellerica, MA.

The authors thank Agnès and Estelle Maublant for their help in the statistical analysis, and Annette Zamora for typing the manuscript.

REFERENCES

1. Karcher G, Bertrand A, Amor M, et al. Qualitative and quantitative comparison of 201-Tl and Tc-99m isonitrile by SPECT in coronary artery disease [Abstract]. *J Nucl Med* 1987; 28:654.
2. Coleman RE, Jaszczak RJ, Cobb FR. Comparison of 180° and 360° data collection in thallium-201 imaging using single-photon emission computerized tomography (SPECT): concise communication. *J Nucl Med* 1982; 23:655–660.
3. Tamaki N, Mukai T, Ishii Y, et al. Comparative study of thallium emission myocardial tomography with 180° and 360° data collection. *J Nucl Med* 1982; 23:661–666.
4. Hoffman EJ. 180° compared with 360° sampling in SPECT. *J Nucl Med* 1982; 23:745–746.
5. Maublant JC. Tl-201 single-photon emission computed tomography (SPECT) [Letter]. *J Nucl Med* 1983; 24:273.
6. Rahimian J, Contino J, Corbus HF, et al. Quantitative evaluation of Tl-201 myocardium SPECT acquisition and processing parameters using a performance index function [Abstract]. *Med Phys* 1984; 11:742.
7. Go RT, Mac Intyre WJ, Houser TS, et al. Clinical evaluation of 360° and 180° data sampling techniques for transaxial SPECT thallium-201 myocardial perfusion imaging. *J Nucl Med* 1985; 26:695–706.
8. Rahimian J, Corbus HF, Touya JJ. Clinical evaluation of 360° and 180° data sampling techniques for transaxial SPECT thallium-201 myocardial perfusion imaging [Letter]. *J Nucl Med* 1986; 27:146–147.
9. Mena I, Philippe L, Darcourt J. Clinical evaluation of 360° and 180° data sampling techniques for transaxial SPECT thallium-201 myocardial perfusion imaging [Letter]. *J Nucl Med* 1986; 27:147.
10. Go RT, Mac Intyre WJ, Houser TJ, et al. Clinical evaluation of 360° and 180° data sampling techniques for transaxial SPECT thallium-201 myocardial perfusion imaging [Letter]. *J Nucl Med* 1986; 27:148–149.
11. Jaszczak RJ, Green KL, Floyd CE, et al. Improved SPECT quantification using compensation for scattered photons. *J Nucl Med* 1984; 25:893–900.
12. Chang LT. A method for attenuation correction in radionuclide computed tomography. *Trans Nucl Sci* 1978; NS-25:638–643.
13. Maublant JC, Cassagnes J, Le Jeune JJ, et al. A comparative study between conventional scintigraphy and emission tomography with thallium-201 in the detection of myocardial infarction: concise communication. *J Nucl Med* 1982; 23:204–208.
14. Burow RD, Pond M, Schafer AW, Becker L. "Circumferential profils": a new method for computer analysis of thallium-201 myocardial perfusion images. *J Nucl Med* 1979; 20:771–777.
15. Tamaki N, Mukai T, Ishii Y, et al. Clinical evaluation of thallium-201 emission myocardial tomography using a rotating gamma camera: comparison with seven pinhole tomography. *J Nucl Med* 1981; 849–855.